Egypt. J. Chem. **Vol. 67** No. 3 pp. 99 - 106 (2024)

Egyptian Journal of Chemistry

http://ejchem.journals.ekb.eg/

Preparation and Evaluation of the Physico-Mechanical Properties of the Magnesium Silicate/Hydroxyapatite Composites

N. El-Mehalawy*, A.M. Hassan, M. Awaad* & S.M. Naga***

**National Research Centre, Refractories, Ceramics and Building materials Department, El-Bohous Str., 12622, Dokki, Giza, Egypt. Fax number, 0020237601877.*
***Zagazig university, Faculty of Engineering, Materials Engineering Department, 44519-Zagazig, Egypt.*

Abstract

Silicate materials have the potential for applications in the biomedical field. This research aims to investigate the effect of incorporating magnesium silicate into the hydroxyapatite (HA) matrix. Four batches of HA; which was synthesized from fish bones; and Mg silicate with various concentrations (5, 10, and 15 %) were prepared by solid-state method. The as-prepared Mg silicate/HA compositions were uniaxially dry-pressed and sintered at different temperatures. The effect of the Mg silicate doping on the physico-mechanical properties of Mg silicate/HA composites was investigated. Results showed that the phase composition of the sintered Mg silicate powder is formed of two phases; forsterite and clinoenstatite. Results for the Mg silicate/HA composite showed the complete disappearance of the HA phase, due to the reaction between Mg silicate and HA. This reaction led to the dissociation of forsterite into clinoenstatite with less Mg content and whitlockite rich in magnesia. Incorporation of Mg^{2+} with hydroxyapatite reduced the bulk density and increased the apparent porosity of the Mg silicate/HA samples. Increasing the Mg silicate content to 10 wt. % enhanced the mechanical properties, while addition of more than 10 wt. % Mg silicate reduced the bending strength and fracture toughness and boosted the Vickers hardness
Keywords: Mg Silicate, Hydroxyapatite, Clinoenstatite, Whitlockite

1. Introduction

Bone grafting is a well-known process requiring materials with an osteoconductive composition and a bioactive behavior similar to that of the bones. Materials such as bioglass and glass–ceramics have been used for bone grafting. Hydroxyapatite (HA), with its biocompatibility, biodegradability, and bioactivity, is one of the most popular calcium phosphate materials used in biomedical applications [1,2]. Porous scaffolds, especially porous HA, are considered as an interesting material for bone grafting. One of the most needed properties of the porous scaffolds is the interconnected pores, as they promote the tissue growth within them [3,4].

The main drawback of the HA scaffolds is their low mechanical properties compared to human bones, which restricts their use in many medical applications [5–9]. Composites are considered good solutions for improving HA mechanical properties, as they do not change the HA bioproperties while enhancing its mechanical behavior [10]. The inert ceramics (such as alumina), the biodegradable ceramics (such as calcium and/or magnesium-based ceramics), glasses, and bioglasses are incorporated with HA to form composites [11–14]. The incorporation of calcium or magnesium silicate into calcium phosphates is considerable of great importance as they are able to enhance cell discrimination and proliferation [15,16]. The Si and Ca ions releasing is the principal reason as they are known as osteoblast developers. Many researchers indicated that bone restoration enhancement was observed on incorporation Ca - Mg silicate to the bone as a result to the affirmative effect of the Mg ions [15, 17, 18]. It was found that if a specific quantity of Mg^{2+} ions is substituted for Ca^{2+} in the lattice of the HA, it will not affect the basic structural characteristics of HA [19–22]. Accordingly, many authors have used forsterite to promote the mechanical and biological properties of the HA. Forsterite Mg and silicon content are crucial

*Corresponding author e-mail: nihal_19832000@yahoo.com
Receive Date: 11 July 2023 Revise Date: 09 September 2023 Accept Date: 12 September 2023
DOI: 10.21608/EJCHEM.2023.222453.8243

for bone regeneration [23–27]. In a study by Mehrjoo et al. [28], they found that Mg^{2+} ions slightly increased the agglomeration of the Mg-HA powder. At the same time, substituting Mg^{2+} ions for HA enhanced both the proliferation rate and gene expression, indicating the favorable role of the Mg^{2+} ions in biomedical applications. A mixture of forsterite (5, 10, and 20 wt.%) and hydroxyapatite was prepared by ball milling and sintering at a temperature between 1100 °C and 1350 °C. The results revealed that the forsterite slightly reacted with HA to produce beta-tricalcium phosphate [ß-$Ca_3(PO_4)_2$]. The transformation phase mentioned above affected the densification parameters and increased the porosity of the sintered bodies. The hardness and fracture toughness of the produced bodies were enhanced because forsterite hindered the HA grain growth [10]. Forsterite was used to prepare forsterite/HA and bioglass/HA composites to coat the 316L stainless steel substrates via either sol–gel or dip coating techniques [29, 30]. The results indicated that both techniques produced a coating layer free from cracks or defects, and the forsterite content positively affected the hardness, fracture toughness, and elastic modulus of the coat.

It was also found that by doping with 5 % magnesium ion; the hydroxyapatite's physico-mechanical properties were improved via the wet precipitation method while doping with higher than 5 % magnesium ion led to a reduction in the relative density [31]. Geng et al., [32] evaluated the effect of incorporating different concentrations of two biological cations; Mg^{2+} and Sr^{2+} into the structure of hydroxyapatite by hydrothermal method and studied their partial substitution for Ca^{2+} in the apatite structure. The co-addition of Mg and Sr to HA enhanced cell growth. The cell proliferation and bioactivity increased on 10Mg20Sr but decreased on 25Mg5Sr, as compared to HA. It was reported that adding Mg and Sr was useful for long-term cell differentiation, especially for 10Mg20Sr.

The effect of doping of $MgSiO_3$ on the 3D Gel-printing hydroxyapatite ceramic composite scaffold has been studied by He et al., [33]. It was found that the porosity and compressive strength of the composite was enhanced. Doping of 3 % $MgSiO_3$ resulted in the highest compressive strength of the composite scaffold of about 93.15 MPa, which authorize it for implantation in high-load parts. Such value is 5.5 times more than that for pure HA scaffold (16.77 MPa). Furthermore, doping with 3 % $MgSiO_3$ possessed better degradability in vitro than the other weight % for $MgSiO_3$. Moradi et al., [34] fabricated a magnesium/nano-hydroxyapatite porous composite with the variable weight of nano-hydroxyapatite (0, 2, 4 and 8 %) by the powder metallurgy method. Better mechanical properties were gained for composites with 2 and 4 wt. % of hydroxyapatites due to the better distribution of hydroxyapatite in the composite matrix. The strength of these composites was about twice and the plateau stress was about three to four times more than that of the pure magnesium. In addition, the elastic modulus of these composites (0.25 GPa) was in the cancellous bone range. Increasing the hydroxyapatite content to 6 and 8 wt. % led to the formation of regions with agglomerated hydroxyapatite particles that acted as a stress concentration agent and reduced the mechanical properties of the composite, as also reported by Feng & Han [35]. In a study of a diopside/forsterite composites fabrication, it was found that increasing the forsterite ratio in the composites led to superior mechanical strength, excellent antibacterial activity, slow degradation and good cell viability. Increasing the diopside content in the composite led to a remarkable improvement in apatite deposition ability [36].

Studying the effect of doping by different MgO concentrations on the mechanical strength and structural and morphological characteristics of the hydroxyapatite derived from eggshell revealed that Mg ions influenced the secondary phase formation of whitlockite and improved the hardness value. The optimum hardness value (HV) of (88.7) was gained with 1 mol. % MgO dopant [37].

This study aims to improve hydroxyapatite's mechanical behavior by incorporating Mg^{2+} into the hydroxyapatite matrix to fabricate Mg silicate/HA composites with appropriate mechanical characteristics and investigate the influence of different Mg ion concentrations doping on the densification, structural and mechanical properties of the obtained composite.

2. Experimental Procedures

2.1. Powder Preparation

Pure nano-HA was produced from fish bones as in previous work of Naga et al. [38]. For Mg_2SiO_4 powder synthesis, predetermined amounts of tetraethyl orthosilicate (TEOS) was hydrolyzed in distelled water and stirred for 2 hours at 80 ºC with the addition of 3 ml nitric acid for peptization. The mixing was continued till a transparent sol was formed and let to cool. Predetermined amount of pure magnesium carbonate was carefully weighed and dissolved gradually in dilute nitric acid to completion and the formation of $MgNO_3$ and then added to the hydrolyzed TEOS. The mixture was continuously stirred at 80 °C till complete gel formation. The prepared gel was dried for 24 h at 110 °C and then calcined at 650 °C to eliminate all nitrate and organic species. It was crushed and ground in a ball mill for 2 h at a speed of 200 rpm. The synthesized powder was sintered at 800 °C, 900 °C, 1000 °C, and 1100 °C with

5 °C/min firing and cooling rates and 1 h at the peak temperature to follow up the phase constitution.

2.2. Preparation of Mg^{2+} Substituted Hydroxyapatite Composites

The HA and Mg silicate powders were dry-mixed in a 3D rotary mixer for 4 hours. Four batches were prepared via ball milling of the mixture at 350 rpm for 4 hours according to the proposed percentage (Table 1). For the formulation of the test samples, the prepared powders were uniaxially pressed at 230 MPa in the form of disks with 13 mm diameter x 5 mm thickness for physical and microstructural examinations and rectangular bars 5×5×60 mm^3 at 300 MPa for the thermal and mechanical properties evaluation. The prepared samples were then sintered in air atmosphere at temperatures between 1200 °C and 1350 °C with a soaking time of 2 h and a firing and cooling rate of 5 °C. To delineate the grain boundary, the tested samples were thermally etched at 50 °C below their sintering temperature with a firing rate of 10 °C/min and a soaking time of 30 min.

Table 1. Batch composition of the studied sintered bodies.

Batch symbol	Hydroxyapatite (mass %)	Mg Silicate (mass %)
A	100	0
B	95	5
C	90	10
D	85	15

2.3. Sample Characterization

+ of ten indentations for each sample. Fracture toughness (K_{IC}) was evaluated using the single edge notched beam technique [39].

3. Results and Discussion

3.1. Phase Composition of the Starting Materials

The XRD patterns of the synthesized Mg silicate powder sintered at 800 °C, 900 °C, 1000 °C, and 1100 °C are illustrated in Fig.1a. Two phases were observed; forsterite (JCPDS: 85-1364) and clinoenstatite (JCPDS: 84-0652). However, the intensity of clinoenstatite peaks had increased by the increasing sintering temperature. An overlap of some peaks for both forsterite and clinoenstatite phases was detected due to the similarity in their crystal lattice spacing. The application of different sintering temperatures was executed to ensure that no other phases than the forsterite and the clinoenstatite were formed by increasing the sintering temperature of the studied composites. The XRD pattern for the pure HA calcinated at 900 °C is shown in Fig. 1b. The figure indicates that HA is composed purely of the Hydroxyapatite phase.

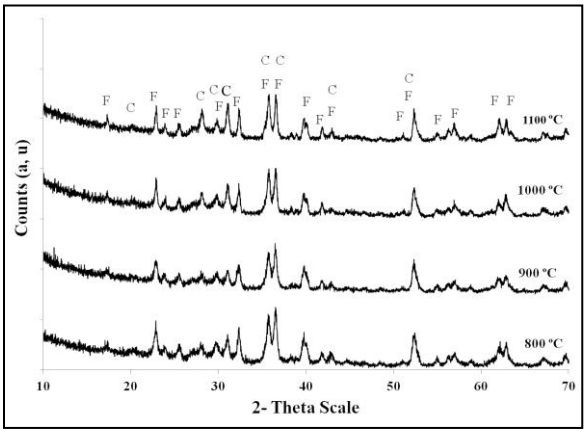

Fig. 1(a). XRD patterns for the synthesized magnesium silicate powder fired at different temperatures (F: forsterite, C: clinoenstatite).

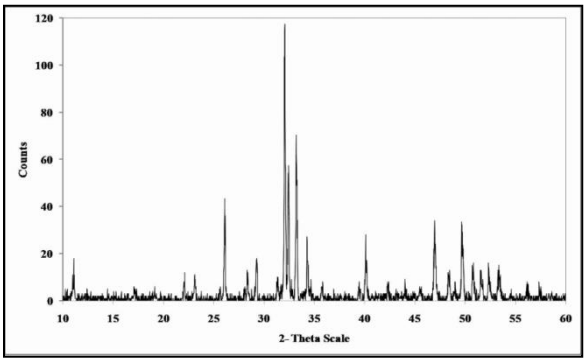

Fig. 1(b). XRD pattern of pure hydroxyapatite**.**

3.2. Physical Properties

The density of hydroxyapatite doped with magnesium ion can be improved at higher sintering temperature. In addition, magnesium was reported as a destabilizing factor in the phase compositions of the co-substituted HA. Incorporation of higher Mg concentration into HA reduces the crystallinity, thermal stability and lattice parameters of HA [32].

The bulk density and apparent porosity of the samples fired at different sintering temperatures as a function of Mg silicate addition are shown in Fig.2 (a, b).

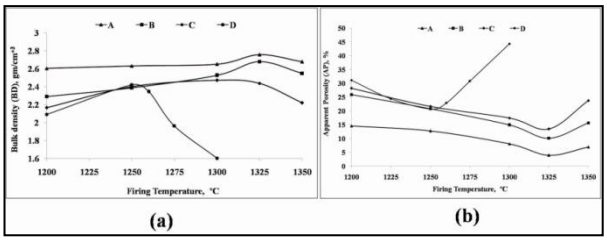

Fig.2. Physical properties for different batch compositions (A: pure HA, B: 95 % HA, C: 90 % HA and D: 85 % HA) fired at different temperatures (a: bulk density; b: apparent porosity**).**

The bulk density of the sintered samples was observed to increase slowly with the sintering temperature. The complete densification of the pure HA (A) and samples containing 5, 10 % Mg- silicate (B and C respectively) was detected at 1325 ºC, while samples containing 15 % Mg- silicate (D) showed densification at 1250 ºC. Additionally, it is observed that the hydroxyapatite samples containing Mg silicate exhibited decreased densities than the pure hydroxyapatite, as shown in Fig. 2 (a). Also, with the increase in the Mg^{2+} concentration, the densification parameters were decreased, which is in agreement with [31].

The apparent porosity displayed a mirror image of the bulk density behavior, Fig. 2 (b). Generally, it decreased with the increase in the sintering temperature until sintering was reached, then it started to increase. The figure indicated that pure HA samples exhibited the lowest apparent porosity compared to bodies containing Mg^{2+} ions. It was also noticed that the increase in the Mg^{2+} ions content increases the bodies' porosity. Although the theoretical density for both the forsterite (3.25 gm/cm^3) and clinoenstatite (3.20 gm/cm^3) is higher than that for HA 3.16 cm^3), Fig.2 (a) illustrates that the magnitude of the bulk density for the Mg silicate/HA composite is less than that for pure HA. It is due to the dissociation of HA to whitlockite, with a density of 3.13 g/cm3, less than that for any of the starting materials, which negatively affected the densification [11].

3.3 Phase Composition

The XRD patterns, Fig.3, showed the complete disappearance of the HA phase in the batch compositions; B (95 % HA) and C (90 % HA) which sintered at 1325 ºC and the composition C (85 % HA) which sintered at 1250 ºC. The only present phases were the whitlockite (JCPDS: 13-0404) and clinoenstatite (JCPDS: 84-0652) phases. It was reported that when Mg^{2+} replaced HA, the high ionic field strength for the Mg^{2+} ions resulting from their small ionic radius weakens the OH^{-}-Ca^{2+} bonds and forms powerful Mg phosphate bonds [40]. Accordingly, the reaction between Mg silicate and HA led to the dissociation of the forsterite into clinoenstatite with less Mg content and whitlockite rich in magnesia. The above-mentioned dissociation process is due to pore formation, which increases the porosity of the sintered bodies with an increase in the Mg silicate content [10].

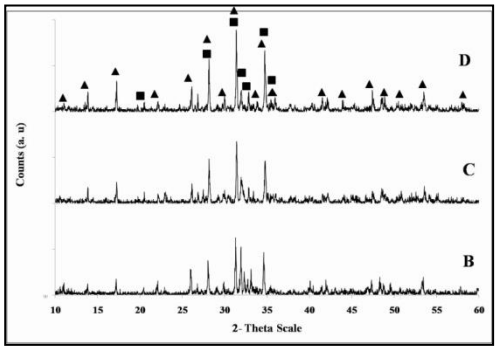

Fig. 3. XRD patterns of the sintered samples (B: 95 % HA, C: 90 % HA and D: 85 %). (▲ : Whitlockite, ■ :Clinoenstatite).

3.4. Microstructural Results

The whitlockite appeared in large particles with sharp boundaries. Some particles had a honeycomb structure, and some were irregular. Clinoenstatite in the form of typical particles or cotton-like agglomerates was scattered over the whitlockite particles or as small rounded particles in the triple junction of the whitlockite particles as appeared in figs.4, 5 and 6.

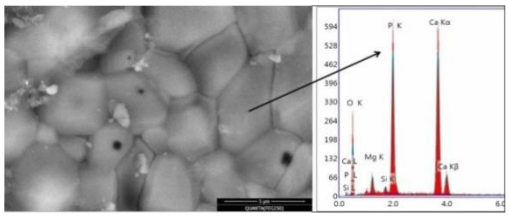

Fig.4. SEM micrograph of sintered bodies containing 5 wt. % Mg silicate, whitlockite and clinoenstatite phases appeared, confirmed with EDS analysis.

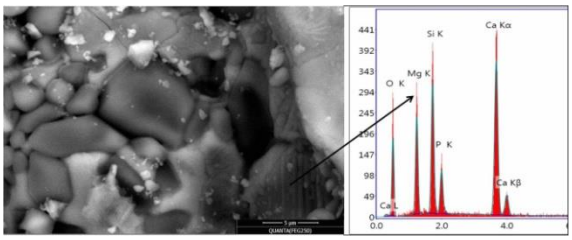

Fig. 5. SEM micrographs of sintered samples containing 10 wt. % Mg silicate showing rod-like clinoenstatite.

Figure 5 exhibited the microstructure of the sintered bodies containing 10 wt. % Mg silicate. The figure shows well crystalline clinoenstatite particles with rod-like grains. They lie parallel to each other on patches. Whereas, the clinoenstatite particles appeared as cotton like shaped that lie on the whitlockite grains, Fig. 6.

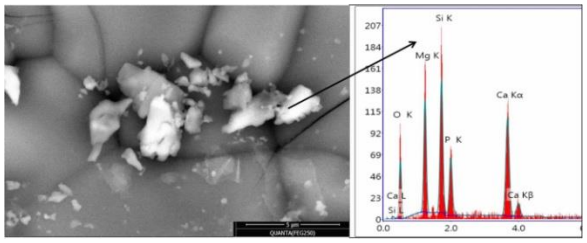

Fig. 6. SEM micrographs of sintered samples containing 15 wt. % Mg silicate showing cotton-like shaped clinoenstatite.

3.5. Mechanical Properties

The fabricated composite exhibited an improvement in the mechanical properties by the incorporation of Mg ions into the HA [41]. Incorporation of Mg ions into HA leads to grain and pore shape modification where, higher content of the Mg ion gives rounder pores, which in turn influences the improvement of the mechanical properties of HA-Mg, as reported by [42].

3.5.1. Bending Strength

Figure 7 indicates that increasing the Mg silicate content up to 10 wt. % enhanced the bending strength of the sintered samples. The bending strength was marginally reduced when the Mg silicate content was increased to 15 wt. %. The addition of Mg silicate in small portions (up to 10 wt. %) could improve the solid interfacial bonds between HA and Mg silicate, which leads to higher reaction sites and better bending strength [43]. Many authors attributed the increase in the bending strength with the increase in the Mg silicate content to the effect of the Mg silicate particles on the movement retardation of the HA dislocations [44], which we considered a second reason for bending strength enhancement. On the other hand, Fig. 7 shows that increasing the Mg silicate to 15 wt. % decreases the bending strength by 1.7 %. This may be due to the negative effect of the increased porosity developed with an increase in the Mg silicate content.

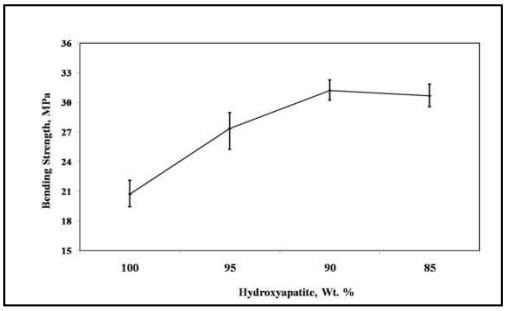

Fig. 7. Bending strength for the sintered Mg silicate/HA composites.

3.5.2. Fracture Toughness

The fracture toughness behaved similarly to the bending strength, Fig.8. It increased with the increase in the Mg silicate content up to 10 wt. %, and then decreased afterward. The enhancement in the fracture strength may be attributed to the spherical pore shape, Fig. 4 (a). It was mentioned that spherical pores enhanced the fracture toughness of the HA composites [42]. The enhancement in the fracture toughness can also be attributed to the formation of strong bonds between the agglomerates during sintering [42]. The increase in the density by the increase in the Mg silicate content is another reason for the enhancement in the fracture toughness of the sintered bodies. The presence of a secondary phase straitens the crack propagation via the stress absorption mechanism and increases the fracture toughness [10]. On the other hand, the spherical pores were approximately disappeared, Fig 5, and the sintering parameters (density and pore size distribution) decreased with the increase in the Mg silicate content to 15 wt. %, which caused a decrease in the fracture toughness.

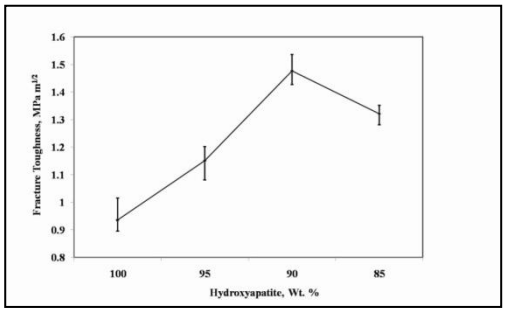

Fig. 8. Fracture toughness for the sintered forsterite/ HA bodies.

3.5.3. Vickers Hardness

Figure 9 shows the effect of Mg silicate wt. % on the Vickers hardness of hydroxyapatite composites. It is noticed that the increase in Mg silicate wt. % enhanced the hardness from 293.4 for pure hydroxyapatite samples to about 515.4 for composites with higher Mg silicate content. The increase in hardness by increasing the Mg silicate content could be related to several factors. The most important in this study is the transfer of the load on the reinforcement particles possessing higher hardness, reducing the stress carried on by the matrix [44].

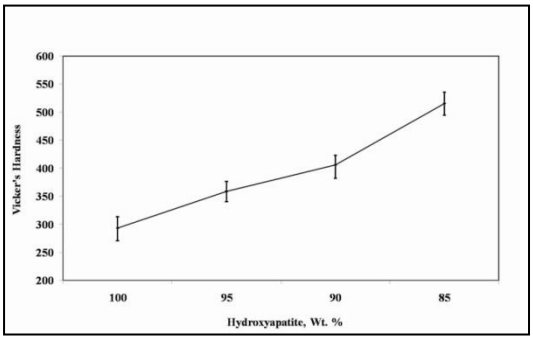

Fig. 9. Vickers hardness of the sintered Mg silicate/HA bodies.

Conclusion

The incorporation of Mg^{2+} into hydroxyapatite samples reduced the densities and increased the porosity of the prepared Mg silicate/HA samples. The more the Mg^{2+} ion content in the composite, the larger the samples porosity obtained. The mechanical properties were improved by increasing the Mg silicate content to 10 wt. %. Both bending strength and fracture toughness values increased to an optimum when Mg silicate content reaches to 10 wt. %. A further increase in the Mg silicate to 15 wt. % reduced the bending strength value. A higher Mg silicate content exhibited the highest Vickers hardness value because the transferring of the load to the reinforcement particles possessing higher hardness reduced the stress carried on by the matrix.

Conflicts of interest

"There are no conflicts to declare".

Formatting of funding sources

No funding sources.

References

[1] Malmberg, P., Nygren, H., 2008. Methods for the analysis of the composition of bone tissue, with a focus on imaging mass spectrometry (TOF-SIMS). Proteomics. 8 [18], 3755-3762. https://doi.org/10.1002/pmic.200800198

[2] Pokhrel, S., 2018. Hydroxyapatite: Preparation, Properties and Its Biomedical Applications. Advances in Chemical Engineering and Science. 8, 225-240. DOI: 10.4236/aces.2018.84016

[3] Lee, K.Y., Park, M., Kim, H.M., Lim, Y.J., Chun, H.J., Kim, H., Moon, S.H., 2006. Ceramic bioactivity: progresses, challenges and perspectives. Annals Biomed. Mat. 1 [2], 31–37. Doi: 10.1088/1748-6041/1/2/R01

[4] Iwasaki, T., Tanaka, Y., Nakamura, M., Nagal, A., Katayama, K., Yamashita, K., 2008. Electrovector effect on bone-like apatite crystal growth on inside pores of polarized porous hydroxyapatite ceramics in simulated body fluid. J. Ceram. Soc. Jap. 116, 23–27. https://doi.org/10.2109/jcersj2.116.23

[5] He, L.H., Standard, O.C., Huang, T.T.Y., Latella, B.A., Swain, M.V., 2008. Mechanical behaviour of porous hydroxyapatite. Acta Biomater. 4 [3], 577-86. https://doi.org/10.1016/j.actbio.2007.11.002

[6] Sopyan, I., Ramesh, S., Nawawi, N.A., Tampieri, A., Sprio, S., 2011. Effects of manganese doping on properties of sol-gel derived biphase calcium phosphate ceramics. Ceram. Int. 37 [8], 3703-3715. https://doi.org/10.1016/j.ceramint.2011.06.033

[7] Ramesh, S., Tan, C.Y., Yeo, W.H., Tolouei, R., Amiriyan, M., Sopyan, I., Teng, W.D., 2011. Effects of bismuth oxide on the sinterability of hydroxyapatite. Ceram. Int. 37 [2], 599-606. https://doi.org/10.1016/j.ceramint.2010.09.041

[8] Ramesh, S., Aw, K.L., Tolouei, R., Amiriyan, M., Tan, C.Y., Hamdi, M., Purbolaksono, J., Hassan, M.A., Teng, W.D., 2013. Sintering properties of hydroxyapatite powders prepared using different methods. Ceram. Int. 39 [1], 111-119. https://doi.org/10.1016/j.ceramint.2012.05.103

[9] Kamalanathan, P., Ramesh, S., Bang, L.T., Niakan, A., Tan, C.Y., Purbolaksono, J., Chandran, H., Teng, W.D., 2014. Synthesis and sintering of hydroxyapatite derived from eggshells as a calcium precursor. Ceram. Int. 40 [10], 16349-16359. https://doi.org/10.1016/j.ceramint.2014.07.074

[10] Ramesh, S., Virik, N.S., Bang, L.T., Niakan, A., Tan, C.Y., Purbolaksono, J., Yap, B.K., Teng, W.D., 2016. Effect of forsterite addition on the densification and properties of hydroxyapatite bioceramic. Journal of Ceramic Processing Research. 17 [1], 30-35.

Corpus ID: 104082438
[11] Aminzare, M., Eskandari, A., Baroonian, M.H., Berenov, A., Hesabi, Z.R., Taheri, M., Sadrnezhaad, S.K., 2013. Hydroxyapatite nanocomposites: Synthesis, sintering and mechanical properties. Ceram. Int. 39 [3], 2197-2206. https://doi.org/10.1016/J.CERAMINT.2012.09.023
[12] Fidancevska, E., Ruseska, G., Bossert, J., Lin, Y.M., Boccaccini, A.R., 2007. Fabrication and characterization of porous bioceramic composites based on hydroxyapatite and titania. Mater. Chem. Phys. 103 [1], 95-100. https://doi.org/10.1016/J.MATCHEMPHYS.2007.01.015
[13] Jun, I.K., Song, J.H., Choi, W.Y., Koh, Y.H., Kim, H.E., Kim, H.W., 2007. Porous hydroxyapatite scaffolds coated with bioactive apatite–wollastonite glass–ceramics. J. Am. Ceram. Soc. 90 [9], 2703-2708. https://doi.org/10.1111/j.1551-2916.2007.01762.x
[14] Kanchana, P., Sekar, C., 2012. Effect of Magnesium on the Mechanical and Bioactive Properties of Biphasic Calcium Phosphate. Journal of Minerals and Materials Characterization and Engineering. 11, 982-988. https://doi.org/10.4236/JMMCE.2012.1110099

[15] Srinath, P., Azeem, P.A., Reddy, K.V., Abdul Azeem, P., Reddy, K.V., 2020. Review on calcium silicate-based bioceramics in bone tissue engineering. Int. J. Appl. Ceram. Technol. 17 [2], 450-2464. https://doi.org/10.1111/ijac.13577
[16] Sadeghzade, S., Liu, J., Wang, H., Li, X., Cao, J., Cao, H., Tang, B., Yuan, H., 2022. Recent advances on bioactive baghdadite ceramic for bone tissue engineering applications: 20 years of research and innovation (a review). Mater. Today Bio. 17, 100473. https://doi.org/10.1016/j.mtbio.2022.100473
[17] Xynos, I.D., Edgar, A.J., Buttery, L.D.K., Hench, L.L., Polak, J.M., 2000. Ionic products of bioactive glass dissolution increase proliferation of human osteoblasts and induce insulin-like growth factor II mRNA expression and protein synthesis. Biochem. Biophys. Res. Commun. 276 [2], 461-465. doi: 10.1006/bbrc.2000.3503
[18] Staiger, M.P., Pietak, A.M., Huadmai, J., Dias, G., 2006. Magnesium and its alloys as orthopedic biomaterials: A review. Biomaterials. 27 [9], 1728-1734. https://doi.org/10.1016/j.biomaterials.2005.10.003
[19] Cai, Y., Zhang, S., Zeng, X., Wang, Y., Qian, M., Weng, W., 2009. Improvement of bioactivity with magnesium and fluorine ions incorporated hydroxyapatite coatings via sol-gel deposition on Ti_6Al_4V alloys. Thin Solid Films. 517 [17], 5347-5351. https://doi.org/10.1016/j.tsf.2009.03.071
[20] Laurencin, D., Almora-Barrios, N., Leeuw, N.H.D., Gervais, C., Bonhomme, C., Mauri, F., Chrzanowski, W. et al., 2011. Magnesium incorporation into hydroxyapatite. Biomater. 32 [7], 1826-1837. https://doi.org/10.1016/j.biomaterials.2010.11.017
[21] Nasr, S., Bouzouita, K., 2011. Sintering behavior of magnesium-substituted fluorapatite powders prepared by hydrothermal method. Bioinorg. Chem. Appl. 4, 453759. https://doi.org/10.1155/2011/453759
[22] Fadev, I.V., Shvorneva, L.I., Barinov, S.M., Orlovskii, V.P., 2003. Synthesis and structure of magnesium-substituted hydroxyapatite. Inorg. Mater. 39, 947-950. DOI:10.1023/A:1025509305805
[23] Ni, S., Chou, L., Chang, J., 2007. Preparation and characterization of forsterite (Mg_2Si0_4) bioceramics. Ceram. Int. 33 [1], 83-88. https://doi.org/10.1016/j.ceramint.2005.07.021
[24] Ni, S., Chang, J., Chou, L., 2008. In vitro studies of novel CaO-SiO_2-MgO system composite bioceramics. J. Mater. Sci. Mater. Med. 19 [1], 359-367. https://doi.org/10.1007/s10856-007-3186-3
[25] Ghomi, H., Jaberzadeh, M., Fathi, M.H. 2011. Novel fabrication of forsterite scaffold with improved mechanical properties. J. Alloy. Compd. 509 [5], 63-68. https://doi.org/10.1016/j.jallcom.2010.10.106
[26] Emadi, R., Tavangarian, F., Esfahani, S.I.R., Sheikhhosseini, A., Kharaziha, M., 2010. Nanostructured forsterite coating strengthens porous hydroxyapatite for bone tissue engineering. J. Am. Ceram. Soc. 93 [9], 2679-2683. https://doi.org/10.1111/J.1551-2916.2010.03817.X
[27] Naga, S.M., Hassan, A.M., Awaad, M., Killinger, A., Gadow, R., Bernstein, A., Sayed, M., 2020. Forsterite/nano-biogenic hydroxyapatite composites for biomedical applications. Journal of Asian Ceramic Societies. 8 [2], 373-386. https://doi.org/10.1080/21870764.2020.1743416
[28] Mehrjoo, M., Javadpour, J., Shokrgzar, M.A., Farokhi, M., Javadian, S., Bonakdar, S., 2015. Effect of magnesium substitution on structural and biological properties of synthetic hydroxyapatite powder. Mater. Express. 5, 41-48. https://doi.org/10.1166/MEX.2015.1205
[29] Sebdani, M.M., Fathi, M.H., 2011. Novel hydroxyapatite-forsterite-bioglass nanocomposite coatings with improved mechanical properties. Journal of Alloys and Compounds. 509, 2273-2276. https://doi.org/10.1016/j.jallcom.2010.10.202
[30] Sebdani, M.M., Fathi, M.H., 2012. Preparation and characterization of hydroxyapatite-forsterite-bioactive glass nanocomposite coatings for

biomedical applications. Ceramics International. 38 [2], 1325-1330. https://doi.org/10.1016/j.ceramint.2011.09.008
[31] Suciu, O., Ioanovici, T., Bereteu, L., 2013. Mechanical Properties of Hydroxyapatite Doped with Magnesium, Used in Bone Implants. Applied Mechanics and Materials. 430, 222-229. DOI:10.4028/www.scientific.net/AMM.430.222
[32] Geng, Z., Wang, R., Li, Z., Cui, Z., Zhu, S., Liang, Y., Liu, Y., Huijing, B., Li, X., Huo, Q., Liu, Z., Yang, X., 2016. Synthesis, characterization and biological evaluation of strontium/magnesium-co-substituted hydroxyapatite. Journal of Biomaterials Applications. 1–12. DOI: 10.1177/0885328216633892
[33] He, J., Shao, H., Lin, T., 2019. Effect of magnesium silicate on 3D gel-printing of hydroxyapatite ceramic composite scaffold. International journal of applied ceramic technology. 16 [2], 494-502. https://doi.org/10.1111/ijac.13133
[34] Moradi, E., Ebrahimian-Hosseinabadi, M., Khodaei, M., Toghyani, S., 2019. Magnesium/Nano-Hydroxyapatite Porous Biodegradable Composite for Biomedical Applications. Materials Research Express. 6 [7], 075408. https://doi.org/10.1088/2053-1591/ab187f
[35] Feng, A., Han, Y., 2011. Mechanical and in vitro degradation behavior of ultrafine calcium polyphosphate reinforced magnesium-alloy composites. Materials & Design. 32 [5], 2813-2820. https://doi.org/10.1016/j.matdes.2010.12.054
[36] Choudhary, R., Venkatraman, S.K., Bulygina, I., Chatterjee, A., Abraham, J., Senatov, F., Kaloshkin, S., Ilyasov, A., Abakumov, M., Knyazeva, M., Kukui, D., Walther, F., Swamiappan, S., 2020. Impact of forsterite addition on mechanical and biological properties of composites. Journal of asian ceramic societies. 8 [4], 1051–1065. https://doi.org/10.1080/21870764.2020.1807695
[37] Noviyanti, A.R., Rahayu, I., Fauzia, R.P. Risdiana, 2021. The effect of Mg concentration to mechanical strength of hydroxyapatite derived from eggshell. Arabian Journal of Chemistry. 14, 103032. https://doi.org/10.1016/j.arabjc.2021.103032
[38] Naga, S.M., El-Maghraby, H.F., Mahmoud, E.M., Talaat, M.S., Ibrahim, A.M., 2015. Preparation and characterization of highly porous ceramic scaffolds based on thermally treated fish bone. Ceram. Int. 41, 15010–15016. https://doi.org/10.1016/J.CERAMINT.2015.08.057
[39] Nishida, T., Hanaki, Y., Pezzotti, G., 2006. Effect of notch-root radius on the fracture toughness of a fine-grained alumina. J. Am. Ceram. Soc. 77 [2], 606–608.https://doi.org/10.1111/j.1151-2916.1994.tb07038.x
[40] Zyman, Z., Tkachenko, M., Epple, M., Polyakov, M., Naboka, M., 2006. Magnesium-substituted hydroxyapatite ceramics. Mat.-Wiss. U. Werkstofftech. 37 [6], 474-477. https://doi.org/10.1002/mawe.200600022
[41] Lala, S., Maity, T.N., Singha, M., Biswas, K., Pradhan, S.K., 2017. Effect of doping (Mg, Mn, Zn) on the microstructure and mechanical properties of spark plasma sintered hydroxyapatites synthesized by mechanical alloying. Ceram. Int. 43, 2389–2397. https://doi.org/10.1016/j.ceramint.2016.11.027.
[42] Veljovic, D.j., Jancic-Hajneman, R., Balac, I., Jokic, B., Putic, S., Petrovic, R., Janackovic, D.j., 2011. The effect of the shape and size of the pores on the mechanical properties of porous HAP-based bioceramics. Ceram. Int. 37 [2], 471–479. https://doi.org/10.1016/j.ceramint.2010.09.014
[43] Kumar, S., Gautam, C., Chauhan, B.S., Srikrishna, S., Yadav, R.S., Rai, S.B., 2020. Enhanced mechanical properties and hydrophilic behavior of magnesium oxide added hydroxyapatite nanocomposite: A bone substitute material for load bearing applications. Ceramics International. 46 [10], 16235-16248. https://doi.org/10.1016/j.ceramint.
[44] Radha, R., Sreekanth, D., 2020. Mechanical and corrosion behavior of hydroxyapatite reinforced Mg-Sn alloy composite by squeeze casting for biomedical applications. Journal of Magnesium and Alloys. 8 [2], 452-460. https://doi.org/10.1016/j.jma.2019.05.010.